Desalination and Water Treatment
www.deswater.com
doi: 10.1080/19443994.2015.1036782

57 (2016) 10378–10390
May

Taylor & Francis
Taylor & Francis Group

Acute impact of dimethyl phthalate on activated sludge nitrification kinetics

Ilke Pala-Ozkok

Faculty of Civil Engineering, Environmental Engineering Department, Istanbul Technical University, Maslak, Istanbul 34469, Turkey, Tel. +90 2122856542; Fax: +90 2122853781; email: palai@itu.edu.tr

Received 17 November 2014; Accepted 25 March 2015

ABSTRACT

This study involved model evaluation of acute impact of dimethyl phthalate (DMP) on substrate utilization kinetics of aerobic nitrifying activated sludge biomass. A laboratory scale fill/draw reactor acclimated to peptone-meat extract mixture, supplying the biomass, was maintained throughout the study and four sets of batch experiments were conducted to determine the acute impact. After nitrification and carbon removal kinetics of the acclimated biomass were determined as a baseline to the acute inhibitory impact studies, 1 g/L DMP concentration was applied. Related experimental data were derived and simulated for model calibration to determine the necessary process kinetics. Model evaluation provided unique information on blockage of nitrification under impact of DMP, and its biological degradation by a fraction of heterotrophic biomass as carbon source at a slower rate than peptone-meat extract mixture.

Keywords: Activated sludge; Modeling; Nitrification; Endocrine disruptor; Dimethyl phthalate

1. Introduction

Phthalic acid esters (PAEs) are endocrine disrupting agents, acting as xenoestrogens [1] that are widely used in different industrial processes [2,3]. They are used in production of plastics, pesticides, pharmaceuticals and cosmetics [4], in addition to being used as additives to fragrances [5]. Even though the acute toxicity of PAEs is low, they were shown to accumulate in aquatic organisms [2,6,7]. These effects of PAEs increased the attention of authorities and scientists on the fate and the effects of these compounds.

Dimethyl phthalate (DMP) is one of the commonly found PAEs in wastewaters, and it is one of the PAEs listed as a priority pollutant by the US Environmental Protection Agency [8]. Major sources of DMP in municipal wastewaters include urban run-offs and industrial and domestic discharges; and concentrations up to mg/L levels may be detected [9]. Perez-Fernandez et al. [10] also reported that DMP was detected in perfumes up to 1,207 ± 43 mg/L concentrations.

In the literature, there are many studies on DMP and its fate in the environment and wastewater treatment facilities, including its biodegradation properties. It has been reported that PAEs can be degraded in aerobic and anaerobic wastewater treatment systems [11]. Wang et al. [12] showed that the protocatechuate pathway followed by ring cleavage is the most common aerobic degradation pathway for the complete mineralization of PAEs. Moreover, Olmez-Hanci et al. [13] reported the 30 min EC_{50} value for DMP as 644 mg/L. However, previous studies also showed that DMPs up to 900 mg/L concentrations did not have any adverse effects on activated sludge

systems [14]. Degradation of DMP during the production of *Bacillus thuringiensis*-based biopesticide has been studied by Brar et al. [15]. The authors determined that up to 500 mg/L DMP concentrations growth of *B. thuringiensis* was not affected. However, 1 and 2 g/L DMP concentrations were shown to have toxic effect on cell growth. Additionally, Ciftci [16] investigated DMP removal under anaerobic mesophilic conditions, applying DMP concentrations ranging from 10 to 1,000 mg/L, where 1,000 mg/L was found to have strong inhibitory effect on methane production.

In this context, the aim of this study was to determine the effect of DMP on activated sludge nitrification process kinetics using respirometry and model evaluation, which was previously never reported. This way, the impact of DMP on all relevant biochemical processes, including microbial growth, hydrolysis, and endogenous respiration, could be assessed separately in terms of related process kinetics and stoichiometry. For this purpose, a synthetic organic substrate was selected as the sole carbon source—peptone–meat extract mixture (*peptone mixture*)—, which resembles domestic and most industrial wastewaters [17], and includes all the chemical oxygen demand (COD) fractions necessary for this evaluation. The study aimed to determine the effect of previously studied toxic concentration of 1 g/L, since this information was non-existent for aerobic mixed microbial culture. Additionally, effect of DMP was studied on nitrification, since it is an important step in wastewater treatment and is one of the most vulnerable stages, which is known to be susceptible to many inhibitory compounds including PAEs [18].

The acute impact of DMP on nitrification was essentially assessed on process kinetics by model evaluation of respirometric data—oxygen uptake rate (OUR) profiles—as well as experimental profiles of different nitrogen fractions. Respirometry measures oxygen consumption under defined conditions [19] and provides oxygen utilization rate (OUR) profiles [20,21]. The obtained OUR profile is used for modeling studies, which incorporate dissolved oxygen, S_O, as the major model component, together with relevant COD and biomass fractions. Additionally, since in single-sludge systems, heterotrophic activity is an important factor for the fate of ammonia nitrogen, it was considered as an integral part of model evaluation on nitrification. Therefore, the model matrix was modified to cover heterotrophic processes and components for carbon removal as well as process kinetics and stoichiometry for nitrification.

2. Materials and methods

2.1. Experimental design

The experimental setup essentially involved (i) a laboratory-scale fill/draw reactor operated, in which both nitrification and denitrification occurred, and (ii) a series batch reactors to determine the effect of DMP (Aldrich W508500, CAS-No:131-11-3) on nitrification kinetics. The fill and draw reactor was utilized to supply acclimated biomass with stable/same characteristics and culture history to the batch experiments. The reactor was operated at steady-state at the sludge age of 10 d. After the initial start-up period, the steady state operation extended and continued at least for a period of three sludge retention times (SRTs); 30 d; to ensure acclimation to the carbon source, peptone mixture. During the steady-state operation, the parent reactor was monitored for COD and volatile suspended solids (VSS) concentrations in the reactors to ensure the existence of stable conditions.

The fill-and-draw reactor was fed with peptone-meat extract mixture (peptone mixture) [22] of 600 mg COD/L concentration. One L of the peptone mixture [22] consisted of 16 g of peptone (Acumedia—Pancreatic Digest of Gelatin (Pepton G) 7182A), 11 g of beef extract (Acumedia—Beef Extract Powder 7228A), 3 g of urea (Acumedia—Urea Agar Base 7226), 0.7 g of NaCl, 0.4 g of $CaCl_2{\cdot}2H_2O$, 0.2 g of $MgSO_4{\cdot}7H_2O$, and 2.8 g of K_2HPO_4. Additionally, a macronutrient solution consisting of K_2HPO_4 (320 g/L) and KH_2PO_4 (160 g/L) and a micronutrient solution ($MgSO_4{\cdot}7H_2O$: 15 g/L, $FeSO_4{\cdot}7H_2O$: 0.5 g/L, $ZnSO_4{\cdot}7H_2O$: 0.5 g/L, $MnSO_4{\cdot}H_2O$: 0.41 g/L, $CaCl_2{\cdot}2H_2O$: 2.65 g/L) were added to the reactor. For each 1,000 mg COD feeding, 20 mL of both macro- and micronutrient solutions were added to the reactor together with the carbon source (peptone mixture). In order to prevent nitrate limitation in the anoxic phase, 100 mg/L nitrate nitrogen was also fed to the reactor. The reactor was kept under anoxic conditions for 7 h and then aerated for 16 h. Additionally, the reactor was kept at idle phase for one hour to ensure sludge settling before the draw phase, which was done once a day, every day. At steady state conditions, the suspended solids (SS) and biomass concentrations for the fill-and-draw reactor were 3,670 ± 110 mg SS/L and 2,400 ± 70 mg VSS/L, respectively. Finally, the effluent COD concentration of the fill-and-draw reactor was 35 ± 1 mg COD/L (94% removal efficiency). Additionally, the fill/draw reactor achieved full nitrification.

Table 1
Characteristics of batch experiments

Runs		Peptone mixture COD (mg/L)	DMP conc. (g/L)	$NO_3^- - N$ conc. (mg/L)	$NH_4^+ - N$ conc. (mg/L)	Biomass conc. (mg VSS/L)	S_0/X_0 (mg COD/mg VSS)	S_0/X_0 (mg N/mg VSS)
Run 1.1	Aerobic control	600	–	100	–	2,400	0.25	–
Run 1.2	Aerobic 1 g/L DMP	400	1	50	–	2,400	0.17	–
Run 2.1	Nitrification control	–	–	–	50	2,420	–	0.02
Run 2.2	Nitrification 1 g/L DMP	–	1	–	50	2,320	–	0.02

2.2. Batch experiments

A series of batch experiments were conducted to visualize and evaluate the acute impact of DMP on the nitrification process. The experiments were started in two sets (Runs 1 and 2), with an acclimated biomass seed taken from the fill-and-draw reactor. Each set involved a parallel batch reactor of 2 L volume, for the respirometric tests for assessing process kinetics and the other for measurements of COD and nitrogen components. Related measurements were made in duplicate and reported as the average value. Each set included a control batch reactor (Runs 1.1 and 2.1) conducted with substrate and biomass only, to determine the biodegradation properties of the peptone mixture, without being exposed to DMP. The other batch reactors in the two sets were conducted with an initial DMP dose of 1 g/L, together with the peptone mixture, to evaluate the acute inhibitory effect of the selected phthalate. It is important to note that the COD equivalent of DMP was also investigated, and it has been determined that 1 g DMP/L had a COD equivalent of 1,000 mg COD/L. Major characteristics of batch experiments are summarized in Table 1.

Batch experiments were started with the biomass seeding alone to obtain the initial endogenous OUR level. Substrate and substrate-DMP mixtures were added on the biomass in the reactor, using suitable S_0/X_0 ratio to avoid oxygen limitation in the respirometric tests and the OUR data was monitored. OUR measurements were performed using a Ra-Combo (Applitek Co., Nazareth, Belgium) continuous respirometer. During batch experiments, each system was monitored by OUR, COD, and nitrogen measurements. Due to the fact that polyhydroxyalkanoates (PHA) and glycogen storage capacity of the main reactor was less than 5%, batch reactors were not monitored for their PHA and glycogen storage properties.

Obtained OUR profiles were used for simulation to determine the kinetic properties of the activated sludge biomass. Simulations were conducted using the AQUASIM program [23], which simulates OUR, COD, and nitrogen data simultaneously.

2.3. Analytical procedures

For soluble COD determination, samples were filtered using 0.45 μm Millipore membrane filters. COD measurements were conducted according to the ISO 6060 procedure [24]. SS and VSS measurements

Table 2
Process rate expressions for autotrophic and heterotrophic processes

Processes	Rate equations
Autotrophs	
[a]Growth of X_{NH}	$\hat{\mu}'_{NH}\frac{S_{NH}}{K_{NH}+S_{NH}}\frac{S_O}{K_{O,NH}+S_O}X_{NH}$
[a]Growth of X_{NO}	$\hat{\mu}'_{NO}\frac{S_{NO2}}{K_{NO}+S_{NO2}}\frac{S_O}{K_{O,NO}+S_O}X_{NO}$
Decay of X_{NO}	$b_{NO}X_{NO}$
Decay of X_{NH}	$b_{NH}X_{NH}$
Heterotrophs	
Growth of X_H	$\hat{\mu}_H\frac{S_S}{K_S+S_S}\frac{S_O}{K_{O,H}+S_O}X_H$
Hydrolysis of S_H	$k_{h1}\frac{S_H/S_HX_HX_H}{K_X+S_H/S_HX_HX_H}X_H$
Hydrolysis of X_S	$k_{h2}\frac{X_S/X_SX_HX_H}{K_{XX}+X_S/X_SX_HX_H}X_H$
Ammonification of S_{ND}	$k_aS_{ND}X_H$
Decay of X_H	b_HX_H
Growth of X_{HDMP}	$\hat{\mu}_{HDMP}\frac{S_S}{K_{SDMP}+S_S}\frac{S_O}{K_{O,H}+S_O}X_{HDMP}$
Hydrolysis of S_{DMP}	$k_{hDMP}\frac{S_{DMP}/S_{DMP}X_{HDMP}X_{HDMP}}{K_{XDMP}+S_{DMP}/S_{DMP}X_{HDMP}X_{HDMP}}X_{HDMP}$
Decay of X_H	$b_{HDMP}X_{HDMP}$

[a]$\hat{\mu}'_{NH}$ and $\hat{\mu}'_{NO}$ are the pH corrected maximum growth rates for X_{NH} and X_{NO}, respectively.

Table 3
Matrix representation of the selected model structure

Process	S_O	S_S	S_P	S_{NH}	S_{ND}	S_{NO2}	S_{NO3}	S_H	S_{DMP}	X_S	X_H	X_{HDMP}	X_{NH}	X_{NO}	X_P	C_{ALK}
Heterotrophic processes for peptone removal																
Growth of X_H	$-\frac{(1-Y_H)}{Y_H}$	$-\frac{1}{Y_H}$		$-i_{NBM}$							1					$-\frac{i_{NBM}}{14}$
Hydrolysis of S_H		1			i_{NSH1}			−1								
Hydrolysis of X_S		1			i_{NSH2}					−1						
Ammonification of S_{ND}				1	−1											$\frac{1}{14}$
Decay of X_H	$-(1-f_{ES}-f_{EX})$		f_{ES}	$i_{NBM}-i_{NXP}f_{EX}-i_{NSP}f_{ES}$							−1				f_{EX}	$\frac{i_{NBM}-i_{NXP}f_{EX}-i_{NSP}f_{ES}}{14}$
Autotrophic processes																
Growth of X_{NH}	$-\frac{(3.43-Y_{NH})}{Y_{NH}}$			$-\frac{1}{Y_{NH}}-i_{NBM}$		$\frac{1}{Y_{NH}}$							1			$-\frac{i_{NBM}}{14}-\frac{2}{14Y_{NH}}$
Growth of X_{NO}	$-\frac{(1.14-Y_{NO})}{Y_{NO}}$			$-i_{NBM}$		$-\frac{1}{Y_{NO}}$	$\frac{1}{Y_{NO}}$							1		$-\frac{i_{NBM}}{14}$
Decay of X_{NH}	$-(1-f_{ES}-f_{EX})$		f_{ES}	$i_{NBM}-i_{NXP}f_{EX}-i_{NSP}f_{ES}$									−1		f_{EX}	$\frac{i_{NBM}-i_{NXP}f_{EX}-i_{NSP}f_{ES}}{14}$
Decay of X_{NO}	$-(1-f_{ES}-f_{EX})$		f_{ES}	$i_{NBM}-i_{NXP}f_{EX}-i_{NSP}f_{ES}$										−1	f_{EX}	$\frac{i_{NBM}-i_{NXP}f_{EX}-i_{NSP}f_{ES}}{14}$
Heterotrophic processes for DMP removal																
Growth of X_{HDMP}	$-\frac{(1-Y_{HDMP})}{Y_{HDMP}}$	$-\frac{1}{Y_{HDMP}}$		$-i_{NBM}$							1					$-\frac{i_{NBM}}{14}$
Hydrolysis of S_{DMP}		1							−1							
Decay of X_{HDMP}	$-(1-f_{ES}-f_{EX})$		f_{ES}	$i_{NBM}-i_{NXP}f_{EX}-i_{NSP}f_{ES}$								−1			f_{EX}	$\frac{i_{NBM}-i_{NXP}f_{EX}-i_{NSP}f_{ES}}{14}$
COD	−1	1	1	–	–	−3.43	−4.57	1	1	1	1	1	1	1	1	–
N	–	–	i_{NSP}	1	1	1	1	i_{NSH1}	–	i_{NSH2}	i_{NBM}	i_{NBM}	i_{NBM}	i_{NBM}	i_{NXP}	–
Ionic charge mole +	–	–	–	$\frac{1}{14}$	–	$-\frac{1}{14}$	$-\frac{1}{14}$	–	–	–	–	–	–	–	–	−1

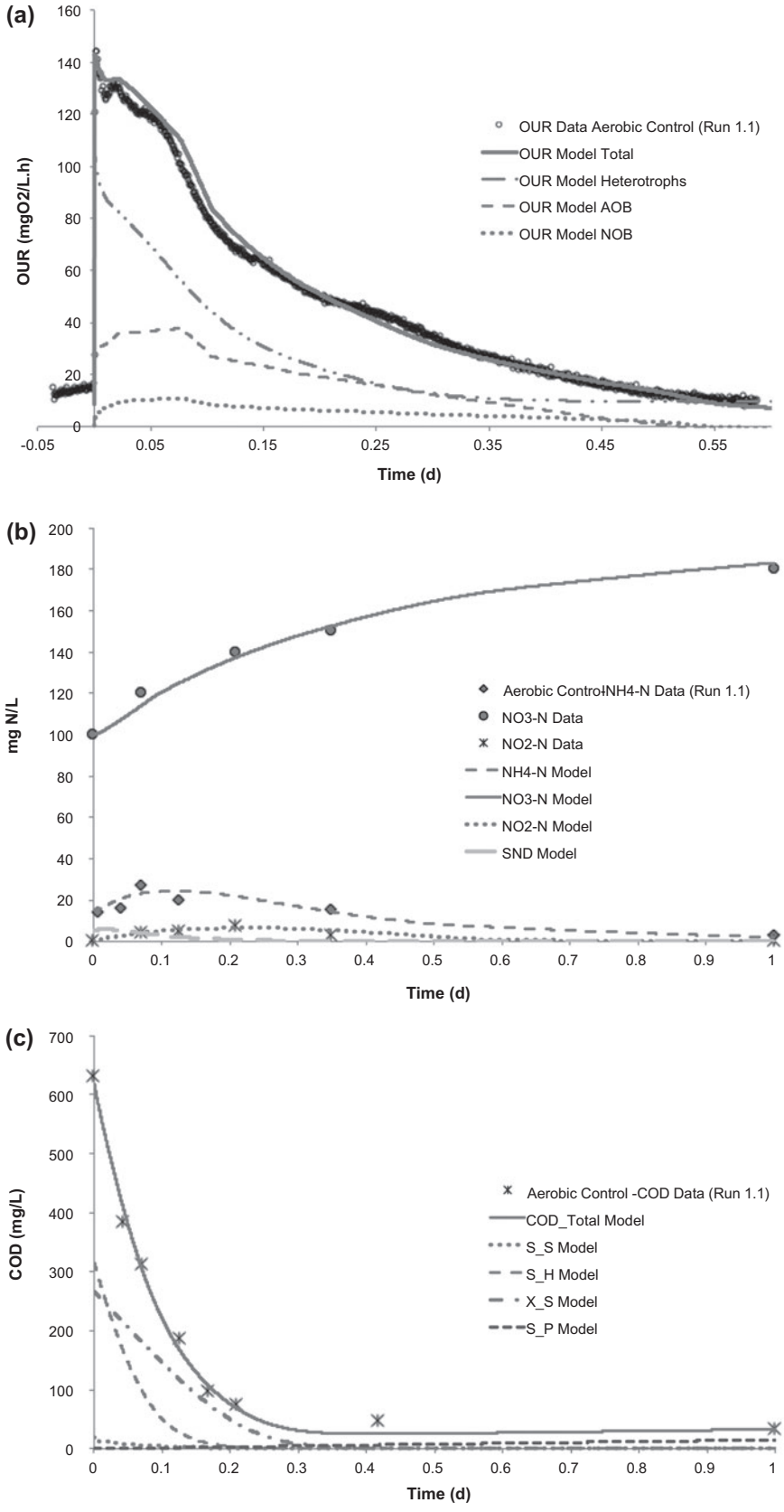

Fig. 1. Model simulation of Run 1.1 (a) OUR profile; (b) Nitrogen profile; (c) COD profile.

were conducted as defined in Standard Methods [25]. During the experiments, Orion 520 A pH meter was used for pH measurements and before each usage of the device, the pH meter was calibrated. Finally, NH_4^+, NO_2^-, and NO_3^- were measured using a Dionex ICS-1500 model Ion Chromatograph.

2.4. Model structure

The adopted model was structured to account for all processes and components necessary for interpreting the inhibitory impact of DMP on different substrate utilization mechanisms involved in the nitrification process. In this context, the model structure included three sub-units. The first one was devoted to nitrification by separately defining microbial processes related to the oxidation of ammonia to nitrite by *ammonia oxidizing bacteria*, X_{NH}, and similarly the oxidation of nitrite to nitrate by *nitrite oxidizing bacteria*, X_{NO}. This part of the model included four processes, the first two of which described the growth of X_{NH} and X_{NO}, whereas the other two processes defined the endogenous decay of the two biomass fractions. The sub-model incorporated six model components, including concentrations of ammonia, S_{NH}, nitrite, S_{NO2}, nitrate, S_{NO3}, the two biomass fractions, X_{NH} and X_{NO} together with alkalinity, $C_{ALK.}$ Due to the fact that autotrophs are more sensitive to changes in environmental conditions in comparison to heterotrophs, rate expressions for microbial growth

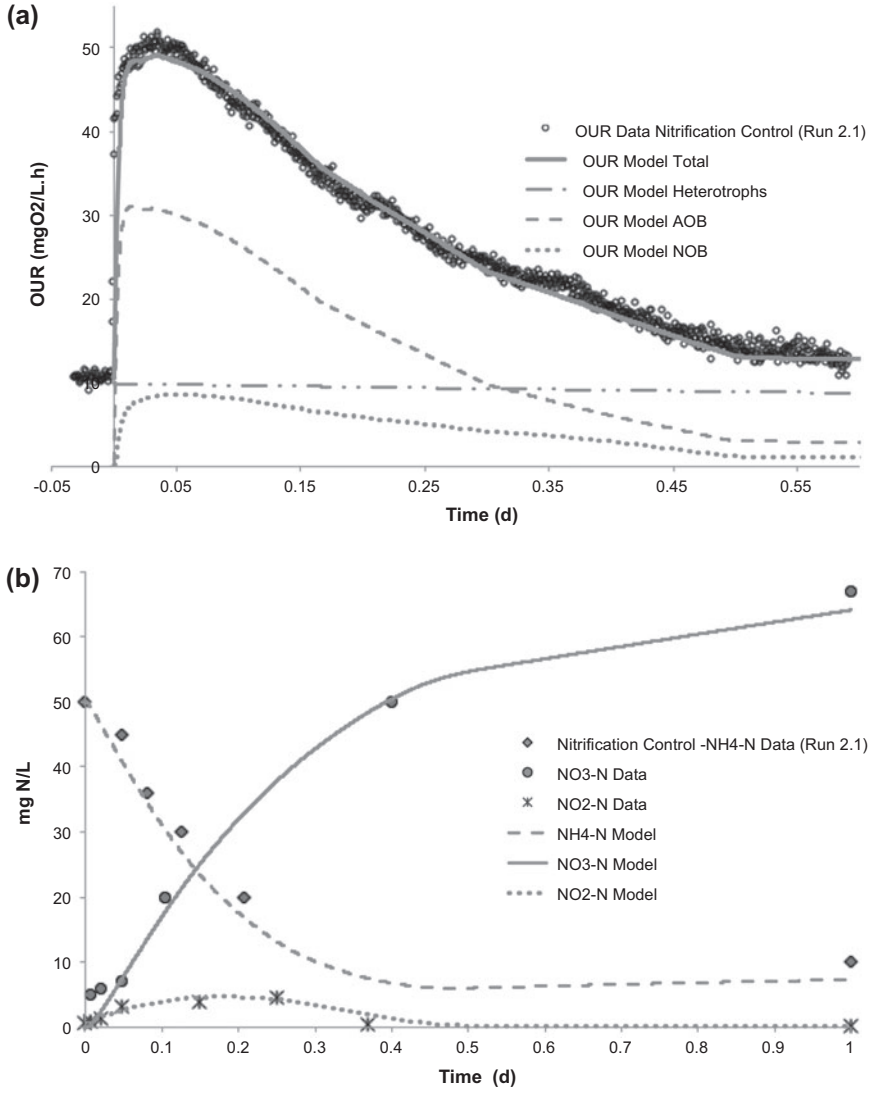

Fig. 2. Model simulation of Run 2.1 (a) OUR profile; (b) Nitrogen profile.

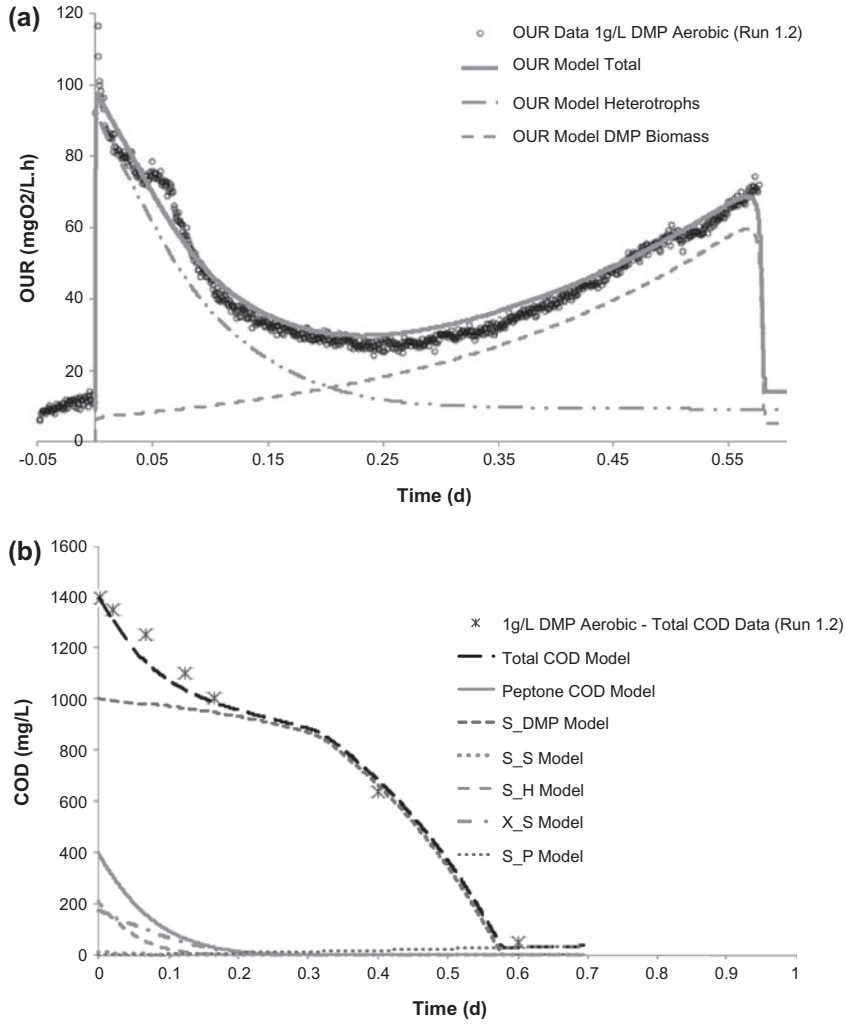

Fig. 3. Model simulation of Run 1.2 (a) OUR profile; (b) COD profile.

were corrected for temperature and pH [26]. The effect of pH on the autotrophic activity was incoroporated into the model structure to apply to both steps of nitrification as previously suggested by Katipoglu-Yazan et al. [27] and by Grunditz and Dalhammar [28].

The other sub-unit was structured to define organic carbon removal. It included the basic template of all similar activated sludge models modified for endogenous respiration [26,29]. It incorporated all the basic components and processes for microbial growth on readily biodegradable COD, S_S, dual hydrolysis of S_H and X_S with different rates [27,30], and endogenous decay of heterotrophic biomass, X_H. The model also accounted for the generation of soluble and particulate microbial products [31], S_P and X_P through endogenous decay. Dissolved oxygen, S_O, is also the most significant model component establishing the functional relationship between the all sub-units of the model. Conversion of organic nitrogen, S_{ND} to ammonia, S_{NH} is also defined by means of heterotrophic ammonification [30].

The third part of the model was structured to describe the biodegradation of DMP, which consisted of two steps. In order to define that process, a hydrolysis step was formulated, in which DMP, S_{DMP}, is broken down to readily biodegradable COD, S_S, selectively utilized by a group of biomass, X_{HDMP}, as the organic carbon source the same way as S_S. The second step of the third part of the model included the endogenous decay of the DMP degrading biomass, X_{HDMP}, which also generates soluble and microbial products, S_P and X_P.

The description of the process rate expressions both for autotrophic and heterotrophic activities are given in Table 2. The basic stoichiometry between

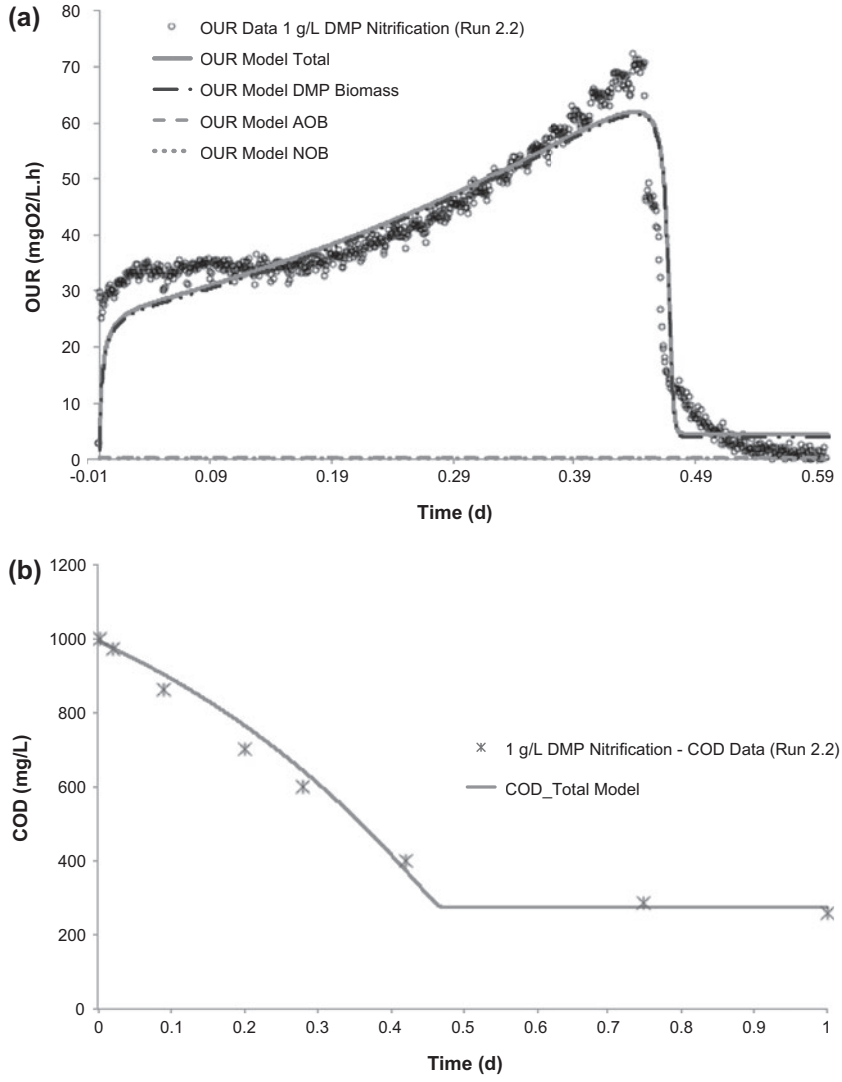

Fig. 4. Model simulation of Run 2.2 (a) OUR profile; (b) COD profile.

model components and processes are defined in Table 3, in the usual matrix format.

It should be noted that OUR profiles are able to produce statistically identifiable results. Moreover, details of parameter identifiability procedure were given in recent studies to be implemented in similar evaluations [21,33]. UNCSIM module proposed by Brun et al. [34], used for the calculation of collinearity indices to define the best identifiable parameter subsets, is applied for parameter identifiability.

Model calibration and evaluation was performed using the AQUASIM program [23]. Model calibration was implemented by means of an iterative calibration protocol, involving manual calibration of model components in each iteration step, and fitting all the model outputs on real time data [35].

3. Results and discussion

3.1. Experimental results

The first batch experiment was carried out to determine the biodegradation kinetics of the peptone mixture by an acclimated activated sludge culture under aerobic conditions (Run 1.1). During this batch experiment, conditions that can be found in single sludge nitrification wastewater treatment systems were simulated, where carbon removal and nitrification take place simultaneously. Moreover, nitrification kinetics were determined in a separate batch of experiment (Run 2.1), in which the biomass was only fed with the nitrogen source so that only autotrophic biomass can remain active.

Table 4
Values of model coefficients assessed by model calibration

Model Parameters	Unit		Run 1.1 Aerobic control	Run 1.2 Aerobic 1 g/L DMP	Run 2.1 Nitrification control	Run 2.2 Nitrification 1 g/L DMP
Autotrophic processes						
Maximum growth rate for X_{NH} (AOB)	$\hat{\mu}'_{NH}$	1/d	1.40	–	1.40	–
Half saturation constant X_{NH}	K_{NH}	mg N/L	0.80	–	0.80	–
Maximum growth rate for X_{NO}(NOB)	$\hat{\mu}'_{NO}$	1/d	0.65	–	0.65	–
Half saturation constant for growth of X_{NO}	K_{NO}	mg N/L	0.50	–	0.50	–
Endogenous decay rate for X_{NH}	b_{NH}	1/d	0.2	–	0.2	–
Endogenous decay rate for X_{NO}	b_{NO}	1/d	0.2	–	0.2	–
Yield coefficient for X_{NH}	Y_{NH}	g COD/g N	0.18	–	0.18	–
Yield coefficient for X_{NO}	Y_{NO}	g COD/g N	0.06	–	0.06	–
Heterotrophic processes for peptone mixture removal						
Maximum growth rate for X_H	$\hat{\mu}_H$	1/d	6	6	–	–
Half saturation constant for growth of X_H	K_S	mg COD/L	24	24	–	–
Maximum hydrolysis rate for S_H	k_{h1}	1/d	6	6	–	–
Hydrolysis half saturation constant for S_H	K_X	g COD/g COD	0.22	0.22	–	–
Maximum hydrolysis rate for X_S	k_{h2}	1/d	1.2	1.2	–	–
Hydrolysis half saturation constant for X_S	K_{XX}	g COD/g COD	0.05	0.05	–	–
Endogenous decay rate for X_H	b_H	1/d	0.2	0.2	0.2	0.2
Yield coefficient for X_H	Y_H	g COD/g COD	0.58	0.58	0.58	0.58
Heterotrophic processes for DMP removal						
Maximum growth rate for X_{HDMP}	$\hat{\mu}_{HDMP}$	1/d	–	4.24	–	4.24
Half saturation constant for growth of X_{HDMP}	K_{SDMP}	mg COD/L	–	3	–	3
Maximum hydrolysis rate for S_{DMP}	k_{hDMP}	1/d	–	6.63	–	6.63
Hydrolysis half saturation constant for S_H	K_{XDMP}	g COD/g COD	–	0.012	–	0.012
Endogenous decay rate for X_{HDMP}	b_{HDMP}	1/d	–	0.32	–	0.32
Yield coefficient for X_{HDMP}	Y_{HDMP}	g COD/g COD	–	0.38	–	0.38

Notes: i_{NBM} = 0.085 g N/g COD; i_{NSp} = 0.01 mg N/mg COD; f_{ES} = 0.05 mg COD/mg COD; f_{EX} = 0.15 mg COD/mg COD [26]; i_{NXp} = 0.03 mg N/mg COD [26]; i_{NSH1}, i_{NSH2} = 0.125 mg N/mg COD [30]; $K_{O,H}$ = 0.16 mg O_2/L, $K_{O,NH}$ = 0.79 mg O_2/L, $K_{O,NO}$ = 0.47 mg O_2/L [32].

The test to determine the aerobic degradation kinetics of the peptone mixture was started with an initial peptone mixture concentration of 600 mg COD/L and 100 mg NO_3^--N/L, simulating the parent reactor. Obtained OUR profile is given in Fig. 1(a), which gives its initial peak at around 140 mg O_2/L h and continues to descent at different rates characterizing different COD fractions present in the peptone mixture. Finally, the OUR profile reached the same endogenous decay level as in the beginning, indicating that all the external carbon and nitrogen sources were depleted by the biomass. As shown in Fig. 1(b), full nitrification was achieved during the test and net amount of 80 mg N/L of nitrate was produced and nitrite nitrogen and

Table 5
Biomass components and COD fractionation assessed by model calibration

State variables		Unit	Run 1.1 Aerobic control	Run 1.2 Aerobic 1 g/L DMP	Run 2.1 Nitrification control	Run 2.2 Nitirification 1 g/L DMP
Total biomass		mg COD/L	3,400	3,400	3,440	3,300
Initial active biomass	X_{H1}	mg COD/L	1,300	1,300	1,500	1,320
Activity		%	38	38	44	40
Initial active ammonia oxidizing biomass	X_{NH1}	mg COD/L	50	50	55	48
Initial active nitrite oxidizing biomass	X_{NO1}	mg COD/L	28	28	30	20
Autotrophic activity	–	%	2	2	2.5	2
Initial active DMP degrading biomass	X_{HDMP1}	mg COD/L	–	50	–	140
Initial amount of ammonia	S_{NH1}	mg N/L	15	10	50	50
Initial amount of nitrate	S_{NO31}	mg N/L	100	50	–	–
Initial amount of organic nitrogen	S_{ND1}	mg N/L	5	3	–	–
Removed amount of DMP	S_{DMP}	mg COD/L	–	200	–	725
Initial amount of biodegradable COD	C_{S1}	mg COD/L	600	400	–	–
Initial amount of readily biodegradable COD	S_{S1}	mg COD/L	18 (3%)	12	–	–
Initial amount of readily hydrolysable COD	S_{H1}	mg COD/L	315 (52.5%)	211	–	–
Initial amount of hydrolysable COD	X_{S1}	mg COD/L	267 (44.5%)	177	–	–

ammonia nitrogen were depleted during the experiment. Additionally, 95% of COD removal was achieved (Fig. 1(c)).

Second batch of experiments were conducted to determine the nitrification kinetics. The experiment was started with an initial dose of 50 mg N/L ammonia. The OUR profile made a peak at around 50 mg O_2/L h and reached the initial endogenous decay level after 0.6 d (Fig. 2(a)). At the end of the experiment, 70 mg N/L nitrate was produced (Fig. 2(b)).

Two more sets of experiments were run to determine the effect of DMP on the kinetics of peptone mixture removal. Third set of experiment (Run 1.2) consisted of 1 g/L DMP addition together with 400 mg COD/L peptone mixture under aerobic conditions (Fig. 3). Finally, during Run 2.2, 1 g/L DMP was added to the system in addition to 50 mg N/L ammonia (Fig. 4). OUR curves obtained from both experimental runs exerted completely different profiles suggesting utilization of DMP by a group of microorganism capable of degrading the substance that are already present in the microbial biomass.

3.2. Model evaluation

Model calibration was done using the experimental data on substrate COD, ammonia, nitrate and nitrite profiles, and OUR profiles. Applicable data were simultaneously calibrated for all sets and the kinetic impact of DMP was determined for all biochemical processes defined by the model. Model coefficients obtained as the result of model calibration studies providing the most appropriate values are indicated in Tables 4 and 5. Additionally, model simulations providing best fits with related experimental data were shown in Figs. 1–4.

Model calibration of the control runs (Run 1.1 and Run 2.1—No DMP addition) resulted in kinetic parameters defining the autotrophic and heterotrophic processes in the reactor providing the best-fit values. As shown in Table 4, model calibration of Run 2.1 provided the maximum specific growth rates of X_{NH} and X_{NO} as 1.4 and 0.65/d, respectively. Additionally, half saturation constants K_{NH} and K_{NO} were also determined to be 0.80 and 0.5 mg N/L, respectively. Results were comparable with previous nitrification

studies conducted with peptone mixture at SRT 10d [27,36]. In this model, calibration study 55 mg COD/L X_{AOB} and 30 mg COD/L X_{NOB} were found to be active nitrifying biomass in the system. The autotrophic activity was 2.5%, and 50 mg N/L ammonia was removed.

In Run 1.1, where both autotrophic and heterotrophic processes were involved, in addition to nitrification kinetics carbon removal kinetics were also determined without the interference of DMP. As a result of the model calibration study, maximum specific growth rate and half saturation constant for the growth of X_H were determined to be 6/d and 24 mg COD/L, respectively. Results were comparable with previous studies conducted with peptone mixture [30,37]. Additionally, three major parts of the peptone mixture were determined (Table 5). Peptone mixture consisted of 3% readily biodegradable fraction, S_S, and 52.5% and 44.5% readily hydrolysable (S_H) and slowly hydrolysable (X_S) COD fractions, respectively, with different hydrolysis rates (Table 4).

3.3. Impact of DMP

The impact of DMP was evaluated with respect to the process kinetics determined by model calibration of Runs 1.1 and 2.1 defining the control reactor. In Run 1.2, the batch reactor was fed with a combination of 400 mg COD/L peptone mixture and 1 g/L DMP in addition to 50 mg N/L nitrate solution. It has been determined that the microbial biomass completely depleted the peptone mixture as the primary carbon source. DMP had no inhibitory impact on the peptone degradation process of the heterotrophic biomass. However, nitrification was fully inhibited. Therefore, no oxygen consumption was observable by the autotrophic biomass, X_{AOB} and X_{NOB}. After the depletion of the peptone mixture in the medium, a fraction of biomass capable of utilizing DMP, X_{HDMP}, degraded the available DMP in the medium, utilizing it as the carbon source, which resulted in an increase in the OUR after 6 h. The area under the curve indicated that the biomass primarily removed 400 mg COD/L peptone mixture and following the depletion of the peptone mixture, the biomass removed 200 mg/L of DMP until the end of the batch experiment.

As indicated in Table 4, in Run 1.2, the maximum growth rate of X_{HDMP}, biomass fraction capable of degrading DMP, was determined to be 4.24/d and the half saturation constant for the growth of X_{HDMP}, K_{SDMP}, 3 mg COD/L, which were comparable with previous studies [38,39]. The kinetics of DMP utilization resembled a hydrolysable compound, which was hydrolyzed at a rate, k_{hDMP}, of 6.63/d and with a half saturation constant, K_{XDMP}, of 0.012 mg COD/L. Additionally, model simulation indicated that the biomass fraction able to degrade DMP, X_{HDMP}, was 50 mg COD/L and had a lower yield coefficient, Y_{HDMP}, of 0.38 g COD/g COD, and higher endogenous decay rate, b_{HDMP}, 0.32/d. Finally, the model simulation indicated that X_{HDMP} removed 200 mg DMP/L, corresponding to a 20% removal efficiency.

Final batch experiment Run 2.2 was also simulated to determine the effect of DMP on nitrification. The batch reactor was fed with a combination of 50 mg N/L ammonia and 1 g/L DMP. As also indicated by the model simulation of Run 1.2, in Run 2.2, nitrification was also completely inhibited with the addition DMP. However, 140 mg COD/L active X_{HDMP} present in the mixed microbial culture removed 725 mg DMP/L (appr. 73% removal efficiency) as there were no other external carbon sources present in the medium. As indicated in Table 4, X_{HDMP} showed the same kinetic properties that were previously determined in Run 1.2.

4. Conclusions

This study presented new and significant results on the acute effects of DMP on the biodegradation kinetics of peptone mixture under nitrifying conditions. The inhibitory effect was mainly blockage of nitrification at the applied concentration; however, results showed that DMP did not have major inhibitory impact on the heterotrophic biomass. Finally, it has been determined that DMP was used as the carbon source and degraded at a slower rate in the absence of an external carbon source by a group of heterotrophic organisms, which have the required enzymes for degradation of DMP.

Acknowledgments

The author would like to thank Dr Tugce Katipoglu-Yazan, Prof. Dr Emine Ubay-Cokgor and Prof. Dr Derin Orhon, as the basic structure of proposed models were taken from PhD Thesis entitled "Evaluation of the Biodegradation Characteristics and Toxicity/Inhibition Effects of Selected Antibiotics on Nitrification Systems".

List of symbols

Ammonia oxidizing bacteria (AOB) — X_{NH}
Nitrate oxidizing bacteria (NOB) — X_{NO}
pH corrected maximum growth rate of maximum growth rate for X_{NH} — $\hat{\mu}_{NH}$
Half saturation constant X_{NH} — K_{NH}
pH corrected maximum growth rate of Maximum growth rate for X_{NO} — $\hat{\mu}_{NO}$
Half saturation constant for growth of X_{NO} — K_{NO}
Endogenous decay rate for X_{NH} — b_{NH}
Endogenous decay rate for X_{NO} — b_{NO}
Yield coefficient for X_{NH} — Y_{NH}
Yield coefficient for X_{NO} — Y_{NO}
Maximum growth rate for X_H — $\hat{\mu}_H$
Half saturation constant for growth of X_H — K_S
Maximum hydrolysis rate for S_H — k_{h1}
Hydrolysis half saturation constant for S_H — K_X
Maximum hydrolysis rate for X_S — k_{h2}
Hydrolysis half saturation constant for X_S — K_{XX}
Endogenous decay rate for X_H — b_H
Yield coefficient for X_H — Y_H
Maximum growth rate for X_{HDMP} — $\hat{\mu}_{HDMP}$
Half saturation constant for growth of X_{HDMP} — K_{SDMP}
Maximum hydrolysis rate for S_{DMP} — k_{hDMP}
Hydrolysis half saturation constant for S_H — K_{XDMP}
Endogenous decay rate for X_{HDMP} — b_{HDMP}
Yield coefficient for X_{HDMP} — Y_{HDMP}
Fraction of nitrogen in biomass — i_{NBM}
Fraction of nitrogen in soluble products from biomass — i_{NSP}
Fraction of biomass converted to S_P — f_{ES}
Fraction of biomass converted to X_P — f_{EX}
Fraction of nitrogen in particulate products from biomass — i_{NXP}
Fraction of nitrogen in S_H — i_{NSH1}
Fraction of nitrogen in X_S — i_{NSH2}
Heterotrophic half saturation coefficient for oxygen, X_H — $K_{O,H}$
Half saturation coefficient of oxygen for X_{NH} — $K_{O,NH}$
Half saturation coefficient of oxygen for X_{NO} — $K_{O,NO}$

References

[1] A. Blom, E. Ekman, A. Johannisson, L. Norrgren, M. Pesonen, Effects of xenoestrogenic environmental pollutants on the proliferation of a human breast cancer cell line (MCF-7), Arch. Environ. Contam. Toxicol. 34 (1998) 306–310.

[2] C.A. Stales, D.R. Peterson, T.F. Parkerton, W.J. Adams, The environmental fate of phthalate esters: A literature review, Chemosphere 35 (1997) 667–749.

[3] H. Fromme, T. Küchler, T. Otto, K. Pilz, J. Müller, A. Wenzel, Occurrence of phthalates and bisphenol A and F in the environment, Water Res. 36 (2002) 1429–1438.

[4] P. Roslev, K. Vorkamp, J. Aarup, K. Frederiksen, P.H. Nielsen, Degradation of phthalate esters in an activated sludge wastewater treatment plant, Water Res. 41 (2007) 969–976.

[5] D.G. Crosby, Environmental Toxicology and Chemistry, Oxford University Press, Oxford, 1998.

[6] S. Nalli, D.G. Cooper, J.A. Nicell, Biodegradation of plasticizers by *Rhodococcus rhodochrous*, Biodegradation 13 (2002) 343–352.

[7] O. Horn, S. Nalli, D. Cooper, J. Nicell, Plasticizer metabolites in the environment, Water Res. 38 (2004) 3693–3698.

[8] United States Environmental Protection Agency. Fate of Priority Pollutants in Publicly Owned Treatment Works. Final report, EPA 440/1-82/303.

[9] J. Vikelsøe, M. Thomsen, E. Johansen, Sources of phthalates and nonylphenols in municipal wastewater. NERI Technical Report No. 225, National Environmental Research Institute, Denmark, 1998.

[10] V. Perez-Fernandez, M.J. Gonzalez, M.A. Garcia, M.L. Marina, Separation of phthalates by cyclodextrin modified micellar electrokinetic chromatography: Quantitation in perfumes, Anal. Chim. Acta 782 (2013) 7–74.

[11] M. Pirsaheb, A.-R. Mesdaghinia, S.J. Shahtaheri, A.A. Zinatizadeh, Kinetic evaluation and process performance of a fixed film bioreactor removing phthalic acid and dimethyl phthalate, J. Hazard. Mater. 167 (2009) 500–506.

[12] J. Wang, P. Liu, Q. Yi, Biodegradation of phthalic acid esters, Chin. J. Environ. Sci. 16 (1995) 26–28.

[13] T. Olmez-Hanci, C. Imren, I. Arslan-Alaton, I. Kabdaşlı, O. Tünay, H2O2/UV-C oxidation of potential endocrine disrupting compounds: A case study with dimethyl phthalate, Photochem. Photobiol. Sci. 8 (2009) 620–627.

[14] T. Ry, The response of activated sludge process of hazardous organic wastes, Hazard. Waste Mater. 8 (1991) 245–256.

[15] S.K. Brar, M. Verma, R.D. Tyagi, J.R. Valéro, R.Y. Surampalli, Concurrent degradation of dimethyl phthalate (DMP) during production of *Bacillus thuringiensis* based biopesticides, J. Hazard. Mater. 171 (2009) 1016–1023.

[16] D.I. Ciftci, Anaerobic treatability of phthalates in domestic solid wastes and treatment sludges, PhD. Thesis, Istanbul Technical University, Turkey, 2012.

[17] G. Insel, O. Karahan, S. Özdemır, L. Pala, T. Katıpoğlu, E. Cokgör, D. Orhon, Unified basis for the respirometric evaluation of ınhibition for activated sludge, J. Environ. Sci. Health A 41 (2006) 1763–1780.

[18] S.N. Dokianakis, M. Kornaros, G. Lyberatos, Impact of five selected xenobiotics on isolated ammonium oxidizers and on nitrifying activated sludge, Environ. Toxicol. 21 (2006) 310–316.

[19] P.A. Vanrolleghem, Principles of respirometry in activated sludge wastewater treatment, in: Proceedings of the International Workshop on Recent Development in Respirometry for Wastewater Treatment Plant Monitoring and Control, Taipei, Taiwan, October 22–23, 2/1–20 (2002).

[20] D. Orhon, E.U. Cokgor, G. Insel, O. Karahan, T. Katipoglu, Validity of monod kinetics at different sludge ages—Peptone biodegradation under aerobic conditions, Bioresour. Technol. 100 (2009) 5678–5686.

[21] A.S. Çığgın, G. Insel, M. Majone, D. Orhon, Respirometric evaluation and modelling of acetate utilization in sequencing batch reactor under pulse and continuous feeding, Bioresour. Technol. 107 (2012) 61–69.
[22] ISO 8192, Water Quality-test for İnhibition of Oxygen Consumption by Activated Sludge, International Standards Organization, 1995.
[23] P. Reichert, J. Ruchti, W. Simon, AQUASIM 2.0, Swiss Federal Institute for Environmental Science and Technology (EAWAG), CH-8600, Duebendorf, Switzerland, 1998.
[24] ISO 6060, Water Quality-determination of the Chemical Oxygen Demand, International Standards Organization, Geneva, 1986.
[25] American Public Health Association/American Water Works Association/Water Environment Federation, Standard Methods for the Examination of Water and Wastewater, twenty-first ed., Washington, DC, 2005.
[26] M. Henze, W. Gujer, T. Mino, M. van Loosdrecht, Activated Sludge Models ASM1, ASM2, ASM2d and ASM3, IWA Publishing, London, 2000.
[27] T. Katipoglu-Yazan, I. Pala-Ozkok, E. Ubay-Cokgor, D. Orhon, Acute impact of erythromycin and tetracycline on the kinetics of nitrification and organic carbon removal in mixed microbial culture, Bioresour. Technol. 144 (2013) 410–419.
[28] C. Grunditz, G. Dalhammar, Development of nitrification inhibition assays using pure cultures of *Nitrosomonas* and *Nitrobacter*, Water Res. 35 (2011) 433–440.
[29] F.G. Babuna, D. Orhon, E.U. Cokgor, G. Insel, B. Yaprakli, Modelling of activated sludge for textile wastewaters, Water Sci. Technol. 38 (1998) 9–17.
[30] T. Katipoglu-Yazan, E. Ubay-Cokgor, G. Insel, D. Orhon, Is ammonification the rate limiting step for nitrification kinetics? Bioresour. Technol. 114 (2012) 117–125.
[31] D. Orhon, N. Artan, Y. Cimsit, The concept of soluble residual product formation in the modelling of activated sludge, Water Sci. Technol. 21 (1989) 339–350.
[32] R. Manser, W. Gujer, H. Siegrist, Consequences of mass transfer effects on the kinetics of nitrifiers, Water Res. 39 (2005) 4633–4642.
[33] E. Cokgor, G. Insel, T. Katipoglu, D. Orhon, Biodegradation kinetics of peptone and 2,6-dihydroxybenzoic acid by acclimated dual microbial culture, Bioresour. Technol. 102 (2011) 567–575.
[34] R. Brun, P. Reichert, H.R. Künsch, Practical identifiability analysis of large environmental simulation models, Water Resour. Res. 37 (2001) 1015–1030.
[35] S.M. Hocaoglu, G. Insel, E.U. Cokgor, D. Orhon, Effect of low dissolved oxygen on simultaneous nitrification and denitrification in a membrane bioreactor treating black water, Bioresour. Technol. 102 (2011) 4333–4340.
[36] T. Katipoglu-Yazan, E.U. Cokgor, D. Derin, Modeling sequential ammonia oxidation kinetics in enriched nitrifying microbial culture, J. Chem. Technol. Biotechnol. 90 (2015) 72–79.
[37] I. Pala-Ozkok, A. Rehman, N. Yagci, E. Ubay-Cokgor, D. Jonas, D. Orhon, Characteristics of mixed microbial culture at different sludge ages: Effect on variable kinetics for substrate utilization, Bioresour. Technol. 126 (2012) 274–282.
[38] S. Sözen, E.U. Çokgör, S. Teksoy Başaran, M. Aysel, A. Akarsubası, I. Ergal, H. Kurt, I. Pala-Ozkok, D. Orhon, Effect of high loading on substrate utilization kinetics and microbial community structure in super fast submerged membrane bioreactor, Bioresour. Technol. 159 (2014) 118–127.
[39] Y. Biros, E.U. Çokgör, N. Yağcı, I. Pala-Ozkok, Z.P. Çakar, S. Sözen, D. Orhon, Effect of acetate to biomass ratio on simultaneous polyhydroxybutyrate generation and direct microbial growth in fast growing microbial culture, Bioresour. Technol. 171 (2014) 314–322.